

Global Energy Optimization of a Light-Duty Fuel-Cell Vehicle

D. Trichet*, S. Chevalier*, G. Wasselynck*, J.C. Olivier*, B. Auvity**, C. Josset**, M. Machmoum*

* IREENA – CRTT 37 bd de l'université BP406 - 44622 Saint-Nazaire CEDEX, France

** Laboratoire de Thermocinétique de Nantes, La Chantrerie, rue Christian PAUC, 44306 Nantes, France

didier.trichet@univ-nantes.fr

Abstract - In this paper, an analytic tank to wheel model of a light-duty fuel-cell vehicle is presented. This model takes into account all the elements of the vehicle along with their interactions. It is used to optimize the velocity profile of the vehicle in order to minimize the energy consumption per kilometer.

Keywords – fuel-cell, power train, energy optimization, analytic model

I. INTRODUCTION

For several years, a light-duty prototype car with extremely low energy consumption is specifically developed to run energetic races [1]. The only energy source of this vehicle is a Proton Exchange Membrane Fuel Cell (PEMFC) [2,3]. Through the 2010 edition of the Shell Eco-marathon competition, on the EuroSpeedway race track, Germany, this vehicle has been recognized as the world most energy efficient car, with an equivalent consumption of only 20.4 ml of unleaded gasoline 95 per 100 km. The structure of the proposed light-duty fuel-cell vehicle is given by Fig. 1. To reach such performances, each element of the vehicle must be optimized, from the mechanical angle (drag coefficient, frontal area, road-wheel friction, weight, etc.) to the electrical architecture (power converter and motor efficiencies, accessories consumption).

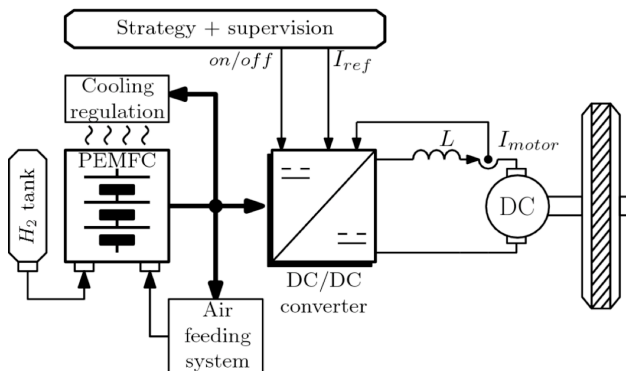


Figure 1. Structure of the light-duty fuel-cell vehicle.

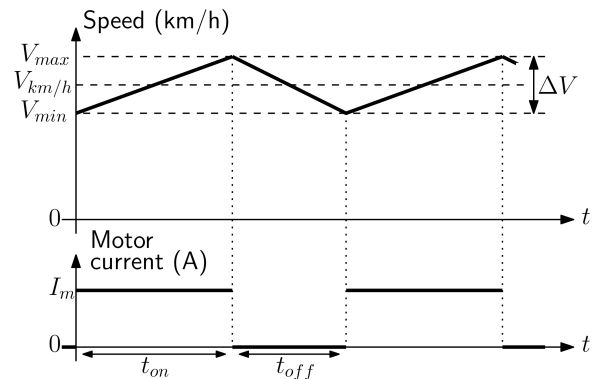


Figure 2. Speed profile of the vehicle.

The fuel-cell is used with a very low current density (close to 1000 A/m²) to target better efficiency (up to 60 % without auxiliaries), i.e. in the activation area of the polarization curve. Working in this area involves control instabilities over long phases of operation [4]. To avoid this problem, the fuel-cell must be stopped during short periods. Thus, in the actual race configuration, the vehicle does not run at a constant speed but with a velocity ripple that assume the same needed average speed, as shown in figure 2. With this velocity profile, the energy is provided only during the acceleration phases (from a minimum to a maximum speed) and is null during free wheel phases (deceleration phase). A judicious choice of the acceleration and deceleration time, maximum and minimum speeds can improve the global energetic performance. The purpose of this paper is to specify the best working points of the vehicle and then the best speed profile. The determination of these working points is based on an analytic tank-to-wheel model of the vehicle linked with an optimization algorithm. This energetic model takes into account: the mechanical part, the efficiency of the power converter, the consumption of the accessories and the polarization curve of the fuel-cell. Due to the extremely low consumption of the car, the model must take into account each element with losses higher than a couple of mW. The computation must also be very fast to match with optimization method's requirements.

The paper is organized as follows: In section II, the analytic tank-to-wheel model is presented which takes taking into account the whole parts of the vehicle. In section III, this model is used to specify the optimal speed profile, given race constraints and rules. Conclusion is given in section IV.

II. ANALYTIC TANK-TO-WHEEL MODEL

In this section, an analytical instantaneous model of the vehicle is proposed. For a given velocity $V_{km/h}$ and motor current I_m , this model gives the instantaneous global efficiency (tank-to-wheel) of the vehicle. Moreover, the various losses and working points of each element can be obtained. Adding the mechanical equations of the vehicle, this model gives the static and dynamic operating points.

A. Analytical instantaneous model

Due to the complexity of the components of the vehicle and their interactions, it is not possible to reduce the modeling to a decoupled study of each element. For instance, the efficiency of the power converter depends on the output voltage of the fuel-cell U_{stack} , itself depends on the power P_{conv} needed by the converter. Therefore, an accurate model of the phenomenon is obtained by a modeling with a strong coupling between elements along with an iterative resolution. The structure of the developed model is presented figure 3.

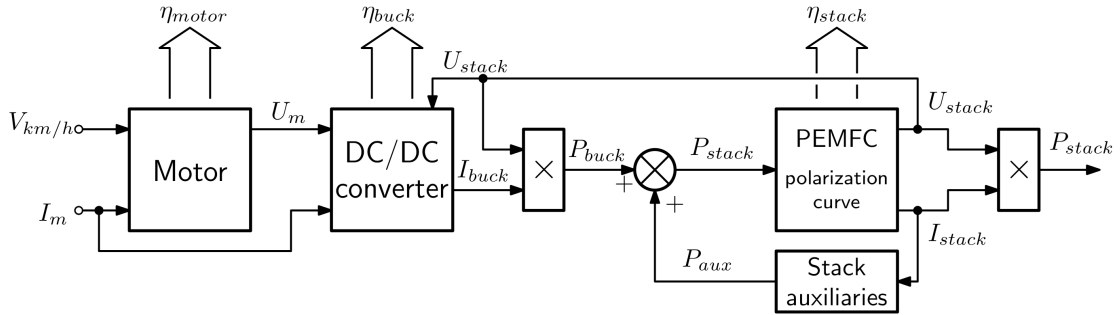


Figure 3. Synoptic of the instantaneous analytic model.

The instantaneous model is made up of four blocks: The fuel-cell stack, the power converter, the propulsion motor and the stack and vehicle auxiliaries. The entries of this model are the instantaneous current I_m of the propulsion motor, speed $V_{km/h}$ of the vehicle and temperature θ of the fuel-cell stack. The outputs are the global and local consumptions of each block and their efficiencies. Entries are directly linked to the mechanical model.

The fuel-cell stack has a power rate of 800 W and is composed of 28 cells connected in series, each of them having an active area of 60 cm². A PEMFC is mainly described by its polarization curve. It gives the voltage level U_{stack} according to the supplied current I_{stack} . The electrochemical equations give a relation between the output voltage U_{stack} and the stack efficiency η_{stack} :

$$\eta_{stack} = \frac{U_{stack}}{N_c} \frac{f}{LHV_{H_2}} \frac{1000}{1} \quad (1)$$

Where f is the Faraday constant (96485.34 C.mol⁻¹), N_c the cells number and LHV_{H_2} the lower heating value of hydrogen. Moreover, the hydrogen flow F_{H_2} (l/s), i.e. the instantaneous hydrogen consumption, is linked to the output current I_{stack} :

$$F_{H_2} = \frac{I_{stack} N_c M_{H_2}}{f \rho_{H_2}} \quad (2)$$

Where ρ_{H_2} is the hydrogen density (0.08988 g/l) and M_{H_2} is the molar mass of hydrogen (1 g.mol⁻¹).

The second element of the power train is the DC/DC buck converter, located between the PEMFC and the DC-motor. This model take into account the losses in the power stage (conduction and commutation losses of MOSFET and diode), in the smooth inductance (copper and magnetic losses), in the wiring and in the small signal electronic control (voltage regulator, current sensor, ...) [1]. The proposed model allows the computation of the converter efficiency η_{buck} , knowing the supplied motor power P_m :

$$\eta_{buck} = \frac{P_m}{P_m + \sum Losses} \quad (3)$$

and

$$\sum Losses = P_{c_mosfet} + P_{c_diode} + P_{sw} + P_{supply} + P_{wiring} + P_{c_ind} + P_{mag} \quad (4)$$

Where P_{c_mosfet} and P_{c_diode} are the conduction losses in the power components, P_{sw} is the switching losses in the power stage [5,6], P_{supply} is the control part consumption, P_{c_ind} and P_{mag} are respectively the copper and magnetic losses in the smooth

inductance [7] and P_{wiring} is the losses in the connection. In the final paper, the computation of these losses will be more described.

The power converter supply a 200 W brushed DC motor with a nominal voltage of 24 V (MAXON® RE50). The choice of this motor is linked to its high efficiency (above 94 %) despite its low power rating. Moreover, the DC motor is iron-less, thus without hysteresis and eddy current losses. The losses in the DC motor are: the dry and viscous friction on the shaft, the Joule losses in the wiring and the voltages drop in the brush.

$$\eta_{motor} = \frac{k_\phi \Omega (I_m - (k_v \Omega + k_d))}{k_\phi \Omega I_m + r I_m^2 + E_b} \quad (5)$$

Where k_ϕ is the torque constant (Nm.A⁻¹), Ω is the rotation speed (rad.s⁻¹), I_m is the motor current (A), k_v is the viscous friction constant (A.rad⁻¹.s), k_d is the dry friction constant (A), r is the wiring resistance (Ω) and E_b is the voltage drop in the brush (V).

In this analytical model, the consumption of the auxiliaries is also taken into account. The power consumption P_{comp} of the air feeding system is function of the supply voltage U_{comp} of the air compressor and is approximated by a third order polynomial. Moreover, the compressor voltage is regulated in order to assume a good stoichiometry in the stack. This stoichiometry depends on the supply current provided by the PEMFC and the temperature.

$$P_{comp} = \alpha_3 U_{comp}^3 + \alpha_2 U_{comp}^2 + \alpha_1 U_{comp} + \alpha_0 \quad (6)$$

With:

$$U_{comp} = f(T, I_{stack}) \quad (7)$$

Concerning the cooling regulation, a bang-bang regulation is used. If the temperature exceeds a threshold, the consumption P_{cool} of the cooling fan is added in the total consumption.

$$\begin{cases} P_{cool} = P_0 & \text{if } T > T_{th} \\ P_{cool} = 0 & \text{if } T \leq T_{th} \end{cases} \quad (8)$$

The consumption of the other auxiliaries (strategy and supervision) is approximated by a constant P_{ctrl} . Finally, the total power consumption of auxiliaries P_{aux} is obtained from equations (6), (7) and (8).

$$P_{aux} = P_{comp} + P_{cool} + P_{ctrl} \quad (9)$$

B. Coupling with mechanical equation

In order to obtain the dynamic and static working points of the vehicle, the mechanical equations are coupled with the model presented in the previous section. To run, the vehicle has to overcome the efforts due to the aerodynamic, the slope, the friction between the wheel and the road. The fundamental law of the mechanic gives the equation to solve:

$$m \frac{dV}{dt} = \eta_{gear} \Gamma_m \frac{G_r}{R} - F_{aero} + F_{slope} + F_{friction} \quad (10)$$

Where m is the mass of the vehicle (kg), V is the vehicle speed (m.s⁻¹), η_{gear} is the efficiency of the freewheel and gear, R is the radius of the wheel (m), G_r is the gear ratio, Γ_m is the motor torque (Nm), F_{aero} is the resistive force due to the aerodynamic losses (N), F_{slope} is the resistive force due to the slope (N) and $F_{friction}$ is the resistive force due to the friction losses (N).

Knowing the mechanical parameters of the vehicle (drag coefficient, mass, gear ratio,...), it is possible to determine a velocity profile for given motor torque and velocity ripple.

C. Results

For each instantaneous working points (motor current and car velocity), the tank-to-wheel efficiency of the car is obtained. Cartography of the iso-efficiency is given figure 4. The static operating points according to wind speed (positive or negative) are added on this figure. For example, to maintain the vehicle at a constant speed of 30 km/h with a 0 km/h wind, it is necessary to supply the motor with a current of 1.9 A. At this point, the global efficiency of the car is equal to 50 %, which is not the most efficient one.

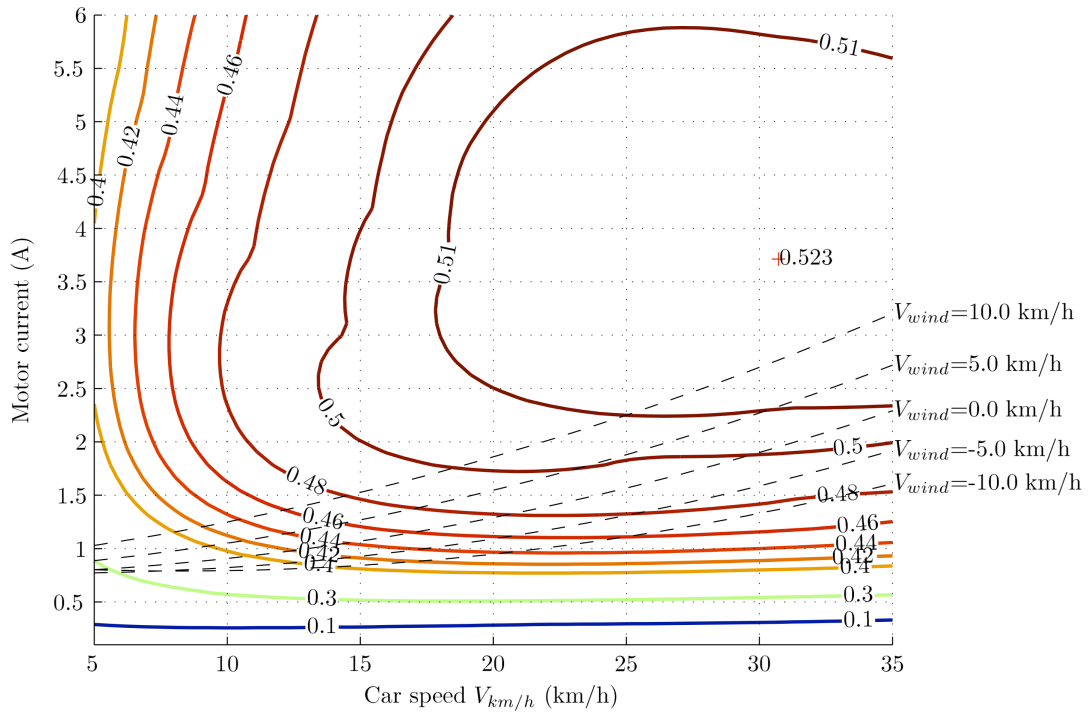


Figure 4. Cartography of iso-efficiency for given car velocity and motor current.

III. OPTIMIZATION

The purpose of the Shell Eco Marathon race is to save a maximum amount of energy for a given mechanical work profile. To achieve this objective, the fuel-cell works in the activation area of the polarization curve in order to obtain the best efficiency (greater than 60 %). However, in this activation area, the voltage tends to decrease slowly according to working time. To overcome this drawback, it is necessary to introduce periodic turn off phases of the fuel-cell. As a consequence, if one wants to assume a constant car velocity it is then necessary to add an energy storage system between the fuel-cell and the motor.

Nevertheless, adding a storage system increases the complexity and the losses of the global structure. Another option, to establish periodic turn off phases without the addition of a storage device, is to work with a velocity ripple, while keeping the same average speed of 30 km/h, as shown figure 2.

The figure 5 shows the increase of mechanical energy need for different velocity ripples. For instance, for a variation speed from 26 to 34 km/h (velocity ripple of 8 km/h), the necessary amount of energy to run the vehicle is one percent upper than the necessary energy for a vehicle running with a constant speed of 30 km/h. Nevertheless, as shown in figure 4, the constant speed strategy operates at a global efficiency of 50.0 %, thus two points fewer than the best efficiency (52.3 % at 3.7 A). This best efficiency point corresponds to a motor current speed upper than the current necessary to maintain a constant velocity. With this current, the car accelerates to reach a stabilized speed of 51 km/h.

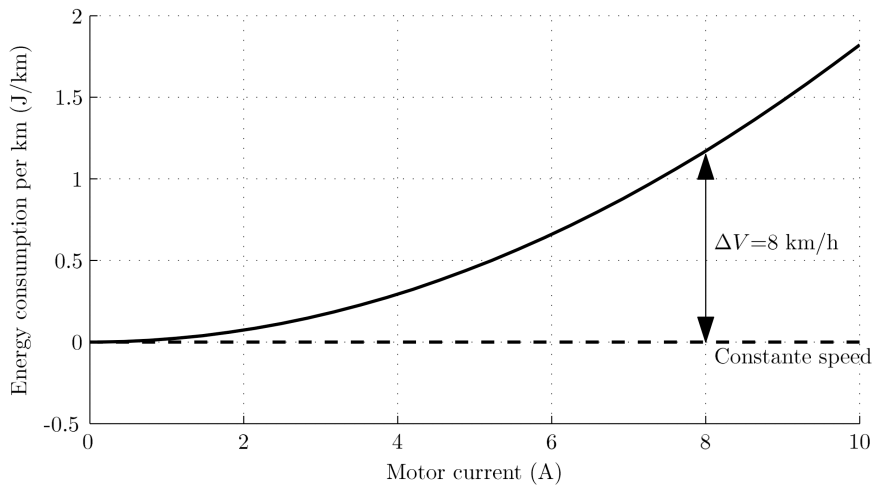


Figure 5. Increase of energy consumption vs velocity ripple, for an average speed of 30 km/h.

The purpose of our study is to determine if the benefit of a greater efficiency compensates the additional energy need due to the velocity ripple. For several speed ripple and several motor currents, the model presented in the previous section permits to determine the energy per km consumption for a given sequence (see figure 2). With a constant speed, the fuel-cell consumes 4980 J of hydrogen per km. The figure 6 shows that a lower consumption is obtained using an acceleration and deceleration strategy, even for large speed variations. A minimal energy consumption of 4783 J/km is obtained, with a velocity ripple of 0.5 km/h around 3.7 A, i.e. the best efficient point observed on figure 4. But, with this speed ripple, the time cycle is 9 s with an off-time of 4 s. This time is too short and need an accurate and fast speed sensor. It is the reason why a speed ripple of 2 km/h is chosen. The energy consumption is only 0.05 % above, but with a time-cycle of 30 s. In the final paper, these results will be extended (influence of wind, gear ratio, ...) and supported through experimental results on a complete race.

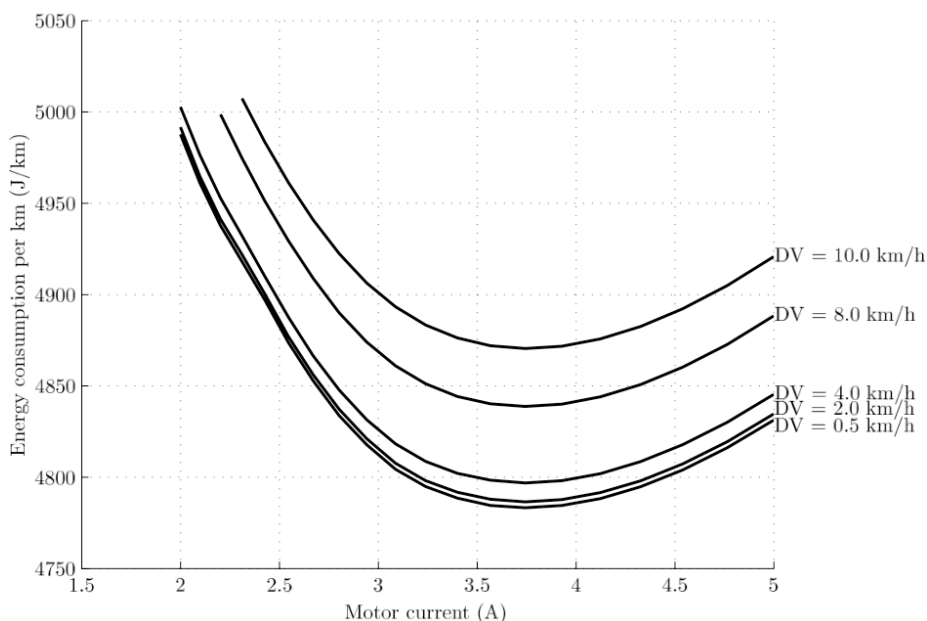


Figure 6. Energy consumption per km vs current motor for several velocity ripple.

IV. CONCLUSION

In this paper, an analytical tank-to-wheel model of a light-duty fuel-cell vehicle is presented. This model takes into account the consumption and the interactions between the various elements of the car. Thus, it permits to find the optimal working points of the vehicle, functions of the imposed motor current and the needed average speed. Furthermore, this model proved that the global efficiency is enhanced by acceleration and deceleration cycles. This particular control sequence also allows a more stable fuel-cell stack, without the addition of an auxiliary storage device.

ACKNOWLEDGMENT

Authors thank the European project ETRERA (Empowering Tunisian Renewable Energy Research Activities) for its support.

REFERENCES

- [1] J.C. Olivier, G. Wasselynck, D. Trichet, B. Auvity, P. Maindr, "Power Source to Wheel Model of a High Efficiency Fuel Cell Based Vehicle", 2010 IEEE Vehicle Power and Propulsion Conference (VPPC 2010), Lilles, France, september 2010.
- [2] R. von Helmolt and U. Eberle, Fuel cell vehicles: status 2007, Journal of Power Sources, 165, 2007, 833-843
- [3] A. Emadi, S.S. Williamson, A. Khaligh, "Power Electronics Intensive Solutions for Advanced Electric, Hybrid Electric, and Fuel Cell Vehicular Power Systems", IEEE Transactions Power Electronics, May 2006, vol, 21, no. 3, pp. 567-577.
- [4] M. M. Mench. "Fuel Cell Engine", Wiley, p. 515, 2005.
- [5] Y. Ren, M. Xu, J. Zhou, F.C. Lee. "Analytical Loss Model of Power MOSFET", IEEE Transactions on Power Electronics, march 2006, vol. 21(2), pages 310 – 319.
- [6] W. Eberle, Z. Zhang, Y.F. Liu, P.C. Sen, "A High Efficiency Synchronous Buck VRM with Current Source Gate Driver", IEEE Power Electronics Specialists Conference (PESC 2007), pp.21-27, 17-21 June 2007.
- [7] C. Oliver, "A New Core Loss Model For Iron Powder Material", Switching Power Magazine, Spring 2002.